

# ANALYTIC ORBIT PROPAGATION FOR TRANSITING CIRCUMBINARY PLANETS

Nikolaos Georgakarakos<sup>1</sup>, Siegfried Eggl<sup>2</sup>

georgakarakosl@hotmail.com

Received \_\_\_\_\_; accepted \_\_\_\_\_

---

<sup>1</sup>New York University Abu Dhabi, Saadiyat Island, PO Box 129188, Abu Dhabi, UAE

<sup>2</sup>IMCCE, Observatoire de Paris, 77 Avenue Denfert-Rochereau, F-75014, Paris, France

## ABSTRACT

The herein presented analytical framework fully describes the motion of coplanar systems consisting of a stellar binary and a planet orbiting both stars on orbital as well as secular timescales. Perturbations of the Runge-Lenz vectors are used to derive short period evolution of the system, while octupole secular theory is applied to describe its long term behaviour. A post Newtonian correction on the stellar orbit is included. The planetary orbit is initially circular and the theory developed here assumes that the planetary eccentricity remains relatively small ( $e_2 < 0.2$ ). Our model is tested against results from numerical integrations of the full equations of motion and is then applied to investigate the dynamical history of some of the circumbinary planetary systems discovered by NASA's Kepler satellite. Our results suggest that the formation history of the systems Kepler-34 and Kepler-413 has most likely been different from the one of Kepler-16, Kepler-35, Kepler-38 and Kepler-64, since the observed planetary eccentricities for those systems are not compatible with the assumption of initially circular orbits.

*Subject headings:* Celestial mechanics, planets and satellites: dynamical evolution and stability, binaries: general

## 1. INTRODUCTION

Many problems in dynamical astronomy and celestial mechanics can be reduced to describing gravitational interactions in hierarchical triple systems. Examples range from asteroid (e.g. Liu et al. 2012) and planetary systems (e.g. Teyssandier et al. 2013) to multi star configurations (e.g. Borkovits et al. 2007) or even systems with compact objects such as black holes (e.g. Blaes et al. 2002). Hierarchical triples consist of a binary system and a third body on a wider orbit. The dynamical behavior of such a configuration can be pictured as the motion of two binaries: the two inner bodies (inner binary) move on a perturbed Keplerian orbit, whereas the third body with the centre of mass of the inner binary form the so-called outer binary. Both orbits exhibit coupled dynamical evolution.

The dynamical behaviour of hierarchical systems, especially the long term (secular) behaviour, has been a subject of intense study in the past. Brouwer (1959), Kaula (1962), Kozai (1962), Lidov (1962), Harrington (1968) and Heppenheimer (1978) are excellent examples of that. Research on the subject has continued throughout the years with Krymowski & Mazeh (1999), Ford et al. (2000), Lee & Peale (2003), Farago & Laskar (2010), Naoz et al. (2013a,b), Leung & Lee (2013), Li et al. (2014) and Liu et al. (2015) being a small sample of recent developments in the subject.

If the system to be modeled is coplanar, then the dynamical evolution of the hierarchical triple is dominated by the time dependent changes in the eccentricity vectors (Laplace-Runge-Lenz vectors) of the inner and outer orbit, as the semi-major axes do not show any secular evolution (e.g. Marchal 1990). Hence, a solution of the differential equations governing the behaviour of the eccentricity vectors allows us to accurately describe the motion of the whole system via closed analytic formulae.

In a series of papers, we focused on the evolution of the inner eccentricity of a hierarchical triple system. In Georgakarakos (2002), we developed a method for measuring

the eccentricity injected to the inner orbit due to the perturbations of the third body. This effect has been known for years (e.g. Mazeh & Shaham 1979), but Georgakarakos (2002) quantified it analytically on both short term and secular timescales for the first time. As those calculations were performed for coplanar and initially circular orbits, they were later on extended to cases where the perturber was on an eccentric orbit (Georgakarakos 2003) as well as for three dimensional cases (Georgakarakos 2004). The initial motivation for that work was closely related to modeling tidal friction in stellar triple systems (e.g. see Kiseleva et al. 1998). Therefore, the systems investigated had comparable masses. Nonetheless, the derived formulae were also tested numerically for planetary mass ratios and remained valid (Georgakarakos 2006). Finally, an improved estimates in the case of coplanar and initially circular orbits were given in Georgakarakos (2009). The analytical formulae for the eccentricity evolution in hierarchical triples have proven to be quite versatile. Chavez et al. (2012) used them to investigate the long term modulation in the lightcurve of the cataclysmic variable FS Aurigae, which was suspected to happen due to the gravitational perturbation of a third body on a much wider orbit. More recently, the limits of various types of habitable zones for a planet in a stellar binary with different spectral type components were investigated analytically as well as numerically (Eggl et al. 2012, 2013).

Boosted by the discovery of several circumbinary planets (e.g. Doyle et al. 2011; Welsh et al. 2012; Orosz et al. 2012; Schwamb et al. 2013; Kostov et al. 2014), the interest in analytical models that describe circumbinary planetary motion has recently grown. In order to create more accurate analytical tools for detection algorithms and planetary formation theories we have to improve first and foremost our description of the eccentricity evolution of planets on circumbinary orbits (also known as P-type orbits). There has been some progress in Georgakarakos (2009) regarding the latter matter, but only hierarchical triple systems on initially circular orbits were treated therein, which may be inadequate in

certain cases. The Kepler-34 system for example has a stellar binary with an eccentricity of  $e \approx 0.52$  (Welsh et al. 2012).

In this paper, we derive analytical expressions for the eccentricity of a relatively light body orbiting a heavier binary, e.g. a planet moving around an eccentric double star. This will allow us to model the dynamical evolution of a circumbinary planet analytically. Since most of the circumbinary planets that have been found via transit searches share more or less the same orbital plane, we will focus on coplanar configurations. Furthermore, we include a post-Newtonian correction into our model, since, in certain cases, General Relativity (GR) may affect the orbit of the inner binary, which in turn influences the evolution of the planetary eccentricity. Our model assumes that the planetary eccentricity is initially circular and it remains valid for low values of the planet’s eccentricity ( $e_2 < 0.2$ ).

The remainder of this article is structured as follows: in section 2, we present the analytical derivation for the eccentricity of the planetary orbit, as well as the expressions for its maximum and averaged value. In section 3, the analytical estimates are compared to results obtained from the numerical integration of the full equations of motion. Next, we discuss the effect of a post-Newtonian correction in our problem (section 4) and we present the formulae for the analytic propagation of the hierarchical triple system (section 5). In section 6, we apply our analytical estimates on six circumbinary planetary systems discovered during the Kepler mission. Finally, we discuss and summarize our results in section 8. A brief description of the variables used in this work can be found in the notation section after the appendix.

## 2. THEORY

We are interested in finding a complete description of the eccentricity vectors of the inner and outer orbit, since those will determine the dynamical evolution of a coplanar hierarchical triple system. As it was stated earlier, we will assume a star-star planet configuration, where all bodies are treated as point-masses. Since the outer body is of planetary size, we can neglect its influence on the amplitude of orbital eccentricity of the inner pair (this will be justified in section 3). Only changes in the direction of the eccentricity vector of the inner orbit will be taken into consideration.

The general way to derive accurate eccentricity estimates that contain long and short periodic contributions has been laid out in Georgakarakos (2003). First, the long term evolution of the eccentricity vector (Laplace-Runge-Lenz vector) is studied by deriving and solving equations of motion that have been averaged over all fast angles. The averaging process via a canonical transformation eliminates all short periodic terms in the eccentricity evolution, so that they do not appear in the final solution. If we want to describe the system's behavior on orbital timescales as well, we can reintroduce short periodic terms by deriving the non-averaged equations for the eccentricity vector. We then eliminate all the components that are already contained in the long term (secular) solution and solve the reduced differential equations. The final solution is a superposition of the short and long periodic solutions of the eccentricity vector.

That kind of approach has been chosen in this work. The secular solutions of the outer eccentricity vector have been constructed from the equations of motion derived from the corresponding canonically averaged Hamiltonians. The short periodic terms, however, had to be themselves split into medium (with periods of the order of the planetary orbital period) and short term (with periods of the order of the stellar orbital period) components in order to allow for an analytic solution. Rejoining the different contributions of the

long, medium and short term solutions leads to the final result as detailed in the following sections.

## 2.1. Calculation of the long term evolution

In order to derive the long-term modulation of the system, we shall use the Hamiltonian formulation (Marchal 1990). For this purpose, we make use of the Delaunay variables, which is a set of canonical variables. For a coplanar three body system they are defined as follows:

$$\begin{aligned}
 L_1 &= mn_1 a_1^2, & l_1, \\
 L_2 &= \mathcal{M} n_2 a_2^2, & l_2, \\
 G_1 &= L_1 \sqrt{1 - e_1^2}, & g_1 = \varpi_1, \\
 G_2 &= L_2 \sqrt{1 - e_2^2}, & g_2 = \varpi_2,
 \end{aligned} \tag{1}$$

where  $a_i$ ,  $e_i$ ,  $\varpi_i$  and  $l_i$  are the semi major axes, the eccentricities, the longitudes of pericenter and mean anomalies of the inner ( $i = 1$ ) and the outer ( $i = 2$ ) orbit respectively.

Furthermore,

$$m = \frac{m_0 m_1}{m_0 + m_1} \quad \text{and} \quad \mathcal{M} = \frac{m_2 (m_0 + m_1)}{M},$$

are the so-called reduced masses, with  $m_0$ ,  $m_1$  and  $m_2$ , being the masses of the stellar binary and planet respectively. The total mass of the system is  $M = \sum_{i=0}^2 m_i$ . Using those variables, the Hamiltonian for a hierarchical triple system reads

$$H = H_0 + H_1 + H_p, \tag{2}$$

where

$$H_0 = -\frac{\mathcal{G}^2 m_0^3 m_1^3}{2(m_0 + m_1) L_1^2} \tag{3}$$

is the Keplerian energy of the inner orbit,

$$H_1 = -\frac{\mathcal{G}^2 (m_0 + m_1)^3 m_2^3}{2M L_2^2} \tag{4}$$

is the Keplerian energy of the outer orbit, and

$$H_p = \mathcal{G}m_2\left(\frac{m_0 + m_1}{R} - \frac{m_0}{r_{02}} - \frac{m_1}{r_{12}}\right), \quad (5)$$

is the perturbing Hamiltonian, with  $r_{02}$  and  $r_{12}$  being the distances between  $m_0$  and  $m_2$  and  $m_1$  and  $m_2$  respectively. Furthermore,  $\mathbf{R}$  is the vector which connects the centre of mass of the inner binary with the third body, while  $\mathbf{r}$  will be denoting the relative position vector of the inner orbit (see Figure 1). Finally,  $\mathcal{G}$  is the gravitational constant.

Since we deal with a hierarchical system and  $r/R$  is small,  $H_p$  can be expressed in terms of Legendre polynomials, giving:

$$H_p = -\frac{\mathcal{G}m_0m_1m_2}{R} \sum_{j=2}^{\infty} M_j \left(\frac{r}{R}\right)^j \mathcal{P}_j(\cos \theta), \quad (6)$$

where  $M_j = \frac{m_0^{j-1} - (-m_1)^{j-1}}{(m_0+m_1)^j}$ ,  $\mathcal{P}_j$  are the Legendre polynomials and  $\theta$ , as seen in Figure 1, is the angle between the  $\mathbf{r}$  and  $\mathbf{R}$  vectors.

The long term behaviour of the system can be obtained when the short period effects in the Hamiltonian are removed by using the Von Zeipel method (e.g. Marchal 1990). The method employs a canonical transformation and details about the derivation can be found elsewhere (Brouwer 1959; Marchal 1990; Krymolowski & Mazeh 1999). The advantage of the Von Zeipel transformation compared to other averaging methods, such as for example the 'scissors method', is that it produces a Hamiltonian which is second order in terms of the masses (although that term will not be used here as its effect is negligible due to the fact that the third body has a planetary mass) and which is complete in terms of the eccentricities. Hence, the Hamiltonian for coplanar orbits averaged over the inner and outer mean anomalies is

$$\langle H \rangle = \langle H_0 \rangle + \langle H_1 \rangle + \langle H_{p2} \rangle + \langle H_{p3} \rangle + \mathcal{O}\left(\frac{r^4}{R^5}\right), \quad (7)$$



with

$$\begin{aligned}
 \langle H_0 \rangle &= -\frac{\mathcal{G}^2 m_0^3 m_1^3}{2(m_0 + m_1)L_{1l}^2} \\
 \langle H_1 \rangle &= -\frac{\mathcal{G}^2(m_0 + m_1)^3 m_2^3}{2ML_{2l}^2} \\
 \langle H_{p2} \rangle &= -\frac{1}{8} \frac{\mathcal{G}^2(m_0 + m_1)^7 m_2^7}{m_0^3 m_1^3 M^3} \frac{L_{1l}^4}{L_{2l}^3 G_{2l}^3} \left(5 - 3 \frac{G_{1l}^2}{L_{1l}^2}\right) \\
 \langle H_{p3} \rangle &= \frac{15}{64} \frac{\mathcal{G}^2(m_0 + m_1)^9 m_2^9 (m_0 - m_1)}{m_0^5 m_1^5 M^4} \frac{L_{1l}^6}{L_{2l}^3 G_{2l}^5} \sqrt{1 - \frac{G_{1l}^2}{L_{1l}^2}} \sqrt{1 - \frac{G_{2l}^2}{L_{2l}^2}} \times \\
 &\quad \times \left(7 - 3 \frac{G_{1l}^2}{L_{1l}^2}\right) \cos(g_{1l} - g_{2l})
 \end{aligned} \tag{8}$$

where the index  $l$  stands for the long term (secular) evolution and  $H_{p2}$  and  $H_{p3}$  come from the  $\mathcal{P}_2$  and  $\mathcal{P}_3$  Legendre polynomials respectively.

Using Delaunay variables, Hamilton's equations assume the following form for a coplanar system:

$$\begin{aligned}
 \frac{dL_{jl}}{dt} &= -\frac{\partial \langle H \rangle}{\partial l_{jl}}, & \frac{dl_{jl}}{dt} &= \frac{\partial \langle H \rangle}{\partial L_{jl}} \\
 \frac{dG_{jl}}{dt} &= -\frac{\partial \langle H \rangle}{\partial g_{jl}}, & \frac{dg_{jl}}{dt} &= \frac{\partial \langle H \rangle}{\partial G_{jl}}, \quad j = 1, 2.
 \end{aligned} \tag{9}$$

Since our Hamiltonian is independent of  $l_{jl}$ , all  $L_{jl}$  are constant. This is a well known result for the averaged problem (e.g. Harrington 1968). Then, keeping in mind that the eccentricity of the stellar orbit remains unchanged due to the fact that the outer body has

a planetary mass, the relevant equations of motion are:

$$\begin{aligned} \frac{dG_{2l}}{dt} &= -\frac{\partial \langle H_{p3} \rangle}{\partial g_{2l}} = -\frac{15 \mathcal{G}^2 (m_0 + m_1)^9 m_2^9 (m_0 - m_1)}{64 m_0^5 m_1^5 M^4} \frac{L_{1l}^6}{L_{2l}^3 G_{2l}^5} \sqrt{1 - \frac{G_{1l}^2}{L_{1l}^2}} \times \\ &\times \sqrt{1 - \frac{G_{2l}^2}{L_{2l}^2}} \left(7 - 3 \frac{G_{1l}^2}{L_{1l}^2}\right) \sin(g_{1l} - g_{2l}) \end{aligned} \quad (10)$$

$$\begin{aligned} \frac{dg_{2l}}{dt} &= \frac{\partial \langle H_{p2} + H_{p3} \rangle}{\partial G_{2l}} = \frac{3 \mathcal{G}^2 (m_0 + m_1)^7 m_2^7}{8 m_0^3 m_1^3 M^3} \frac{L_{1l}^4}{L_{2l}^3 G_{2l}^4} \left(5 - 3 \frac{G_{1l}^2}{L_{1l}^2}\right) - \\ &- \frac{15 \mathcal{G}^2 (m_0 + m_1)^9 m_2^9 (m_0 - m_1)}{64 m_0^5 m_1^5 M^4} \frac{L_{1l}^6}{L_{2l}^3} \sqrt{1 - \frac{G_{1l}^2}{L_{1l}^2}} \left(7 - 3 \frac{G_{1l}^2}{L_{1l}^2}\right) \times \\ &\times \left( \frac{5 \sqrt{1 - \frac{G_{2l}^2}{L_{2l}^2}}}{G_{2l}^6} + \frac{1}{L_{2l}^2 G_{2l}^4 \sqrt{1 - \frac{G_{2l}^2}{L_{2l}^2}}} \right) \cos(g_{1l} - g_{2l}) \end{aligned} \quad (11)$$

$$\begin{aligned} \frac{dG_{1l}}{dt} &= \frac{\partial \langle H_{p2} + H_{p3} \rangle}{\partial G_{1l}} = \frac{3 \mathcal{G}^2 (m_0 + m_1)^7 m_2^7}{4 m_0^3 m_1^3 M^3} \frac{L_{1l}^2 G_{1l}}{L_{2l}^3 G_{2l}^3} + \\ &- \frac{15 \mathcal{G}^2 (m_0 + m_1)^9 m_2^9 (m_0 - m_1)}{64 m_0^5 m_1^5 M^4} \frac{L_{1l}^5}{L_{2l}^3 G_{2l}^5} \sqrt{1 - \frac{G_{2l}^2}{L_{2l}^2}} \frac{G_{1l}}{\sqrt{L_{1l}^2 - G_{1l}^2}} (13 - \\ &- 9 \frac{G_{1l}^2}{L_{1l}^2}) \cos(g_{1l} - g_{2l}) \end{aligned} \quad (12)$$

If we replace the Delaunay variables from equations (1) with the corresponding orbital elements and use  $e_{21l} = e_{2l} \cos g_{2l}$  and  $e_{22l} = e_{2l} \sin g_{2l}$ , the above system becomes:

$$\begin{aligned} \frac{de_{21l}}{dt} = & -\frac{3}{8} \frac{\sqrt{\mathcal{G}M}m_0m_1a_{1l}^2}{(m_0+m_1)^2a_{2l}^{\frac{7}{2}}(1-e_{2l}^2)^2} (2+3e_{1l}^2)e_{22l} + \\ & + \frac{15\sqrt{\mathcal{G}M}m_0m_1(m_0-m_1)a_{1l}^3}{64(m_0+m_1)^3a_{2l}^{\frac{9}{2}}(1-e_{2l}^2)^3} e_{1l}(4+3e_{1l}^2) [(1+4e_{22l}^2-e_{21l}^2)\sin g_{1l} + \\ & + 5e_{21l}e_{22l}\cos g_{1l}] \end{aligned} \quad (13)$$

$$\begin{aligned} \frac{de_{22l}}{dt} = & \frac{3}{8} \frac{\sqrt{\mathcal{G}M}m_0m_1a_{1l}^2}{(m_0+m_1)^2a_{2l}^{\frac{7}{2}}(1-e_{2l}^2)^2} (2+3e_{1l}^2)e_{21l} + \\ & + \frac{15\sqrt{\mathcal{G}M}m_0m_1(m_0-m_1)a_{1l}^3}{64(m_0+m_1)^3a_{2l}^{\frac{9}{2}}(1-e_{2l}^2)^3} e_{1l}(4+3e_{1l}^2) [(-1+e_{22l}^2-4e_{21l}^2)\cos g_{1l} - \\ & - 5e_{21l}e_{22l}\sin g_{1l}] \end{aligned} \quad (14)$$

$$\begin{aligned} \frac{dg_{1l}}{dt} = & \frac{3}{4} \frac{\sqrt{\mathcal{G}}m_2a_{1l}^{\frac{3}{2}}\sqrt{1-e_{1l}^2}}{(m_0+m_1)^{\frac{1}{2}}a_{2l}^3(1-e_{2l}^2)^{\frac{3}{2}}} - \frac{15\sqrt{\mathcal{G}}m_2(m_0-m_1)a_{1l}^{\frac{5}{2}}e_{2l}\sqrt{1-e_{1l}^2}}{64(m_0+m_1)^{\frac{3}{2}}a_{2l}^4e_{1l}\sqrt{1-e_{2l}^2}} (4+ \\ & + 9e_{1l}^2)\cos(g_{1l}-g_{2l}). \end{aligned} \quad (15)$$

Since the planetary orbit is initially circular and its eccentricity is expected to remain small, we neglect terms of order  $O(e_{2l}^2)$  in the above equations and we also keep the dominant term in the equation for the stellar pericentre. As a result, the equations of motion assume the following form:

$$\frac{de_{21l}}{dt} = -K_1e_{22l} + K_2\sin g_{1l}, \quad (16)$$

$$\frac{de_{22l}}{dt} = K_1e_{21l} - K_2\cos g_{1l}, \quad (17)$$

$$\frac{dg_{1l}}{dt} = K_3, \quad (18)$$

where

$$\begin{aligned} K_1 &= \frac{3\sqrt{\mathcal{G}M}m_0m_1a_{1l}^2}{8(m_0+m_1)^2a_{2l}^{\frac{7}{2}}}(2+3e_{1l}^2) \\ K_2 &= \frac{15\sqrt{\mathcal{G}M}m_0m_1(m_0-m_1)a_{1l}^3}{64(m_0+m_1)^3a_{2l}^{\frac{9}{2}}}e_{1l}(4+3e_{1l}^2) \\ K_3 &= \frac{3\sqrt{\mathcal{G}}m_2a_{1l}^{\frac{3}{2}}\sqrt{1-e_{1l}^2}}{4(m_0+m_1)^{\frac{1}{2}}a_{2l}^3} \end{aligned} \quad (19)$$

are constants.

The above system of differential equations can be solved analytically and the solution is

$$\begin{aligned} e_{21l}(t) &= C_1 \cos K_1 t + C_2 \sin K_1 t + \frac{K_2}{K_1 - K_3} \cos K_3 t \\ e_{22l}(t) &= C_1 \sin K_1 t - C_2 \cos K_1 t + \frac{K_2}{K_1 - K_3} \sin K_3 t, \end{aligned} \quad (20)$$

for the planetary orbit, where  $C_1$  and  $C_2$  are constants of integration. For the stellar orbit we get

$$g_{1l} = K_3 t, \quad (21)$$

where we have assumed without loss of generality that the initial longitude of pericenter of the inner orbit is zero. Consequently, the components of the eccentric vector of the stellar orbit become

$$\begin{aligned} e_{11l}(t) &= e_1 \cos g_{1l} = e_1 \cos (K_3 t) \\ e_{12l}(t) &= e_1 \sin g_{1l} = e_1 \sin (K_3 t), \end{aligned} \quad (22)$$

So far our results are in agreement with other authors, e.g. Moriwaki & Nakagawa (2004), Demidova & Shevchenko (2014).

## 2.2. Calculation of the short and mid term evolution

Having the long term solution for the eccentricity evolution of our system at our disposal, we now proceed to derive equations for the mid and short periodic terms. Once again, we use the Jacobi decomposition of the three body problem to describe the motion of the system (see Figure 1). In that context, the equation of motion of the outer body is:

$$\ddot{\mathbf{R}} = -\mathcal{G}M \left( \mu_0 \frac{\mathbf{R} + \mu_1 \mathbf{r}}{|\mathbf{R} + \mu_1 \mathbf{r}|^3} + \mu_1 \frac{\mathbf{R} - \mu_0 \mathbf{r}}{|\mathbf{R} - \mu_0 \mathbf{r}|^3} \right) = \mathcal{G}M \frac{\partial}{\partial \mathbf{R}} \left( \frac{\mu_0}{|\mathbf{R} + \mu_1 \mathbf{r}|} + \frac{\mu_1}{|\mathbf{R} - \mu_0 \mathbf{r}|} \right) \quad (23)$$

with

$$\mu_i = \frac{m_i}{m_0 + m_1}, \quad i = 0, 1.$$

Once more, since we work with a hierarchical triple system and the third body is assumed to be at considerable distance from the inner binary, implying that  $r/R$  is small, the inverse distances in equation (23) can be expressed in terms of Legendre polynomials as

$$\frac{1}{|\mathbf{R} + \mu_1 \mathbf{r}|} = \frac{1}{R} \sum_{n=0}^{\infty} \left( -\frac{\mu_1 r}{R} \right)^n \mathcal{P}_n(\cos \theta), \quad (24)$$

and

$$\frac{1}{|\mathbf{R} - \mu_0 \mathbf{r}|} = \frac{1}{R} \sum_{n=0}^{\infty} \left( \frac{\mu_0 r}{R} \right)^n \mathcal{P}_n(\cos \theta). \quad (25)$$

Expanding to second order and making the substitution

$$\cos \theta = \frac{\mathbf{r} \cdot \mathbf{R}}{rR},$$

the equation of motion of the outer binary becomes

$$\ddot{\mathbf{R}} = \mathcal{G}M \left\{ -\frac{\mathbf{R}}{R^3} + \mu_0 \mu_1 \left[ 3 \frac{(\mathbf{r} \cdot \mathbf{R}) \mathbf{r}}{R^5} - \frac{15}{2} \frac{(\mathbf{r} \cdot \mathbf{R})^2 \mathbf{R}}{R^7} + \frac{3}{2} \frac{r^2 \mathbf{R}}{R^5} \right] \right\} \quad (26)$$

Using the Runge-Lenz vector of the outer orbit we can obtain an expression for the eccentricity. Hence:

$$\begin{aligned} \mathbf{e}_2 &= -\frac{\mathbf{R}}{R} + \frac{1}{\mathcal{G}M} (\dot{\mathbf{R}} \times \mathbf{h}) \Rightarrow \\ \dot{\mathbf{e}}_2 &= -\frac{\dot{\mathbf{R}}}{R} + \frac{\dot{R}}{R^2} \mathbf{R} + \frac{1}{\mathcal{G}M} [2(\dot{\mathbf{R}} \cdot \ddot{\mathbf{R}}) \mathbf{R} - (\mathbf{R} \cdot \ddot{\mathbf{R}}) \dot{\mathbf{R}} - (\mathbf{R} \cdot \dot{\mathbf{R}}) \ddot{\mathbf{R}}], \end{aligned} \quad (27)$$

where  $\mathbf{h} = \mathbf{R} \times \dot{\mathbf{R}}$ .

Substituting equation (23) into equation (27) and assuming that the eccentricity remains small (and hence neglecting the term  $\mathbf{R} \cdot \dot{\mathbf{R}}$ ), we obtain:

$$\dot{\mathbf{e}}_{2sm} = \frac{m_0 m_1}{(m_0 + m_1)^2} \left[ 6 \frac{(\mathbf{r} \cdot \mathbf{R})(\mathbf{r} \cdot \dot{\mathbf{R}})}{R^5} \mathbf{R} + \frac{9}{2} \frac{(\mathbf{r} \cdot \mathbf{R})^2}{R^5} \dot{\mathbf{R}} - \frac{3}{2} \frac{r^2}{R^3} \dot{\mathbf{R}} \right], \quad (28)$$

where the indices  $s$  and  $m$  refer to short and medium period terms as explained earlier.

Now, the Jacobi vectors can be represented as  $\mathbf{r} = a_1(\cos E_1 - e_1, \sqrt{1 - e_1^2} \sin E_1)$  and  $\mathbf{R} = a_2(\cos l_2, \sin l_2)$ , where  $a_1$ ,  $e_1$ ,  $E_1$ , are the semi-major axis, the eccentricity and the eccentric anomaly of the inner orbit, while  $a_2$  and  $l_2$  are the semi major-axis and the mean anomaly of the outer orbit respectively. Substituting for  $\mathbf{r}$  and  $\mathbf{R}$  in equation (28), we acquire for the rate of change of the componets of the outer eccentric vector:

$$\begin{aligned} \dot{e}_{21sm}(t) &= \frac{m_0 m_1}{(m_0 + m_1)^{\frac{4}{3}} M^{\frac{2}{3}} X^{\frac{4}{3}}} \frac{n_2}{X^{\frac{4}{3}}} \left[ 6 [(\cos E_1 - e_1) \cos l_2 + \sqrt{1 - e_1^2} \sin E_1 \sin l_2] \times \right. \\ &\quad \times \left[ -(\cos E_1 - e_1) \sin l_2 + \sqrt{1 - e_1^2} \sin E_1 \cos l_2 \right] \cos l_2 - \frac{9}{2} [(\cos E_1 - e_1) \cos l_2 + \sqrt{1 - e_1^2} \sin E_1 \sin l_2]^2 \sin l_2 + \frac{3}{2} (1 - e_1 \cos E_1)^2 \sin l_2 \left. \right] \\ \dot{e}_{22sm}(t) &= \frac{m_0 m_1}{(m_0 + m_1)^{\frac{4}{3}} M^{\frac{2}{3}} X^{\frac{4}{3}}} \frac{n_2}{X^{\frac{4}{3}}} \left[ 6 [(\cos E_1 - e_1) \cos l_2 + \sqrt{1 - e_1^2} \sin E_1 \sin l_2] \times \right. \\ &\quad \times \left[ -(\cos E_1 - e_1) \sin l_2 + \sqrt{1 - e_1^2} \sin E_1 \cos l_2 \right] \sin l_2 + \frac{9}{2} [(\cos E_1 - e_1) \cos l_2 + \sqrt{1 - e_1^2} \sin E_1 \sin l_2]^2 \cos l_2 - \frac{3}{2} (1 - e_1 \cos E_1)^2 \cos l_2 \left. \right], \end{aligned} \quad (29)$$

where  $X$  is the period ratio of the two orbits.

By using equations (29), we are now able to obtain the short period terms for the evolution of the planetary eccentric vector. This will be done in two steps. First, we average the above equations over the fast motion and then we integrate over time:

$$\begin{aligned} e_{21m}(t) &= \frac{1}{16} \frac{m_0 m_1}{(m_0 + m_1)^{\frac{4}{3}} M^{\frac{2}{3}} X^{\frac{4}{3}}} \frac{1}{X^{\frac{4}{3}}} \left[ 12 \cos l_2 + e_1^2 (33 \cos l_2 + 35 \cos 3l_2) \right] + C_{e_{21m}} \\ e_{22m}(t) &= \frac{1}{16} \frac{m_0 m_1}{(m_0 + m_1)^{\frac{4}{3}} M^{\frac{2}{3}} X^{\frac{4}{3}}} \frac{1}{X^{\frac{4}{3}}} \left[ 12 \sin l_2 + e_1^2 (3 \sin l_2 + 35 \sin 3l_2) \right] + C_{e_{22m}}. \end{aligned} \quad (30)$$

Here,  $C_{e_{21m}}$  and  $C_{e_{22m}}$  are constants of integration. In a second step we add higher frequency terms by integrating equations (29) with respect to time. During that process, any terms that appear and have already been taken into consideration (given by equations (30)) are

removed. Integrating by parts yields a power series solution in terms of  $1/X$ . By keeping the largest term in that power series we finally end up with the following short term equations for the eccentric vector of the planetary orbit:

$$\begin{aligned} e_{21s}(t) &= \frac{m_0 m_1}{(m_0 + m_1)^{\frac{4}{3}} M^{\frac{2}{3}} X^{\frac{7}{3}}} P_1(t) + C_{e_{21s}} \\ e_{22s}(t) &= \frac{m_0 m_1}{(m_0 + m_1)^{\frac{4}{3}} M^{\frac{2}{3}} X^{\frac{7}{3}}} P_2(t) + C_{e_{22s}}, \end{aligned} \quad (31)$$

with  $P_1(t)$  and  $P_2(t)$  given in the Appendix. Combining equations (30) and (31) we find formulae for all non-secular contributions:

$$\begin{aligned} e_{21sm}(t) &= \frac{m_0 m_1}{(m_0 + m_1)^{\frac{4}{3}} M^{\frac{2}{3}} X^{\frac{4}{3}}} \left[ \frac{3}{4} \cos l_2 + e_1^2 \left( \frac{33}{16} \cos l_2 + \frac{35}{16} \cos 3l_2 \right) + \frac{P_1(t)}{X} \right] + C_{e_{21sm}} \\ e_{22sm}(t) &= \frac{m_0 m_1}{(m_0 + m_1)^{\frac{4}{3}} M^{\frac{2}{3}} X^{\frac{4}{3}}} \left[ \frac{3}{4} \sin l_2 + e_1^2 \left( \frac{3}{16} \sin l_2 + \frac{35}{16} \sin 3l_2 \right) + \frac{P_2(t)}{X} \right] + C_{e_{22sm}}. \end{aligned} \quad (32)$$

We would like to point out here that  $a_1$ ,  $a_2$  and  $e_1$  have been treated as constants in the above calculations.

### 2.3. Complete solution of the eccentricities

We can now combine equations (20) and (32) in order to obtain the total solution for the outer eccentricity. As in the case of the inner eccentricity, this is done by substituting the constants of integration in the short period solution with the expressions for the secular evolution:

$$\begin{aligned} e_{21}(t) &= e_{21s}(t) + e_{21m}(t) + e_{21l}(t) - C_{e_{21sm}} \\ e_{22}(t) &= e_{22s}(t) + e_{22m}(t) + e_{22l}(t) - C_{e_{22sm}}. \end{aligned} \quad (33)$$

The constants in equation (33) are determined by the fact that we assume the outer eccentricity to be initially zero, i.e.

$$e_{21}(t_0) = e_{22}(t_0) = 0 \quad (34)$$

which eventually leads to

$$\begin{aligned}
 e_{21}(t) &= \frac{m_0 m_1}{(m_0 + m_1)^{\frac{4}{3}} M^{\frac{2}{3}} X^{\frac{4}{3}}} \left[ \frac{3}{4} \cos l_2 + e_1^2 \left( \frac{33}{16} \cos l_2 + \frac{35}{16} \cos 3l_2 \right) + \frac{P_1(t)}{X} \right] + \\
 &\quad C_1 \cos K_1 t + C_2 \sin K_1 t + \frac{K_2}{K_1 - K_3} \cos K_3 t \\
 e_{22}(t) &= \frac{m_0 m_1}{(m_0 + m_1)^{\frac{4}{3}} M^{\frac{2}{3}} X^{\frac{4}{3}}} \left[ \frac{3}{4} \sin l_2 + e_1^2 \left( \frac{3}{16} \sin l_2 + \frac{35}{16} \sin 3l_2 \right) + \frac{P_2(t)}{X} \right] + \\
 &\quad C_1 \sin K_1 t - C_2 \cos K_1 t + \frac{K_2}{K_1 - K_3} \sin K_3 t,
 \end{aligned} \tag{35}$$

where

$$\begin{aligned}
 C_1 &= -\frac{m_0 m_1}{(m_0 + m_1)^{\frac{4}{3}} M^{\frac{2}{3}} X^{\frac{4}{3}}} \left[ \frac{3}{4} \cos l_{20} + e_1^2 \left( \frac{33}{16} \cos l_{20} + \frac{35}{16} \cos 3l_{20} \right) + \right. \\
 &\quad \left. + \frac{P_1(t_0)}{X} \right] - \frac{K_2}{K_1 - K_3}
 \end{aligned} \tag{36}$$

$$\begin{aligned}
 C_2 &= \frac{m_0 m_1}{(m_0 + m_1)^{\frac{4}{3}} M^{\frac{2}{3}} X^{\frac{4}{3}}} \left[ \frac{3}{4} \sin l_{20} + e_1^2 \left( \frac{3}{16} \sin l_{20} + \frac{35}{16} \sin 3l_{20} \right) + \right. \\
 &\quad \left. + \frac{P_2(t_0)}{X} \right].
 \end{aligned} \tag{37}$$

The quantities  $K_i$  have been defined in equations (19) and  $l_{20}$  is the initial planetary mean anomaly. The evolution of the eccentricity of the inner orbit is given by equations (22).

## 2.4. Maximum and average squared outer eccentricity

We can also obtain an estimate for the maximum value the outer eccentricity is bound to reach during its evolution assuming it was initially zero. This is achieved by doing some algebraic manipulations and by maximizing trigonometric functions in equations (20) and (32). Eventually we obtain:

$$\begin{aligned}
 e_2^{max} &= e_{2sm}^{max} + e_{2l}^{max} \\
 &= \frac{m_0 m_1}{(m_0 + m_1)^{\frac{4}{3}} M^{\frac{2}{3}} X^{\frac{4}{3}}} \left[ \frac{3}{2} + \frac{17}{2} e_1^2 + \frac{1}{X} \left( 3 + 19e_1 + \frac{21}{8} e_1^2 - \frac{3}{2} e_1^3 \right) \right] \\
 &\quad + \frac{2K_2}{K_1 - K_3}.
 \end{aligned} \tag{38}$$



Averaging equations (35) over time we obtain the following expression (excluding the short period terms):

$$\begin{aligned}
 \langle e_2^2 \rangle_t &= \langle e_{21}^2(t) + e_{22}^2(t) \rangle_t = \frac{m_0^2 m_1^2}{(m_0 + m_1)^{\frac{8}{3}} M^{\frac{4}{3}} X^{\frac{8}{3}}} \frac{1}{8} \left[ \frac{9}{8} + \frac{27}{8} e_1^2 + \frac{887}{64} e_1^4 + \right. \\
 &\quad \left. + \frac{75}{16} e_1^2 + e_1^4 \left( \frac{225}{32} \cos 2l_{20} + \frac{525}{128} \cos 4l_{20} \right) \right] + \\
 &\quad + \frac{m_0 m_1}{(m_0 + m_1)^{\frac{4}{3}} M^{\frac{2}{3}} X^{\frac{4}{3}}} \frac{K_2}{K_1 - K_3} \left[ \frac{3}{2} \cos l_{20} + e_1^2 \left( \frac{33}{8} \cos l_{20} + \right. \right. \\
 &\quad \left. \left. + \frac{35}{8} \cos 3l_{20} \right) \right] + 2 \left( \frac{K_2}{K_1 - K_3} \right)^2. \tag{39}
 \end{aligned}$$

If equations (35) are averaged over both time and initial angles, we find the most compact expression for the averaged square outer eccentricity:

$$\begin{aligned}
 \langle e_2^2 \rangle &= \langle e_{21}^2(t) + e_{22}^2(t) \rangle = \frac{m_0^2 m_1^2}{(m_0 + m_1)^{\frac{8}{3}} M^{\frac{4}{3}} X^{\frac{8}{3}}} \frac{1}{8} \left[ \frac{9}{8} + \frac{27}{8} e_1^2 + \frac{887}{64} e_1^4 - \right. \\
 &\quad \left. - \frac{975}{64} \frac{1}{X} e_1^4 \sqrt{1 - e_1^2} + \frac{1}{X^2} \left( \frac{225}{64} + \frac{6619}{64} e_1^2 - \frac{26309}{512} e_1^4 - \frac{393}{64} e_1^6 \right) \right] + \\
 &\quad + 2 \left( \frac{K_2}{K_1 - K_3} \right)^2. \tag{40}
 \end{aligned}$$

### 3. NUMERICAL TESTING

In order to test the validity of our analytical estimates, we integrated the full equations of motion numerically. For that purpose, we used the symplectic integrator with time transformation developed by Mikkola (1997), specially designed to integrate hierarchical triple systems. The code uses standard Jacobi coordinates, i.e. it calculates the relative position and velocity vectors of the inner and outer orbit at every time step. Those were used to generate orbital elements of the stellar and planetary orbits.

We investigated systems with nine different mass combinations. Stellar masses were chosen such as  $m_1/(m_0 + m_1) = 0.5, 0.3, 0.1$ . The planetary masses we used were such that

$m_2/(m_0 + m_1) = 10^{-2}, 10^{-3}, 10^{-6}$ , i.e. we chose Earth-like, Jovian and brown dwarf like companions. The eccentricity ranged from 0 to 0.9, while for the semimajor axis the range was between one and 12 times the critical semi-major axis as given in Holman & Wiegert (1999), who studied the stability of planetary orbits in binary star systems by performing numerical simulations in the framework of the planar elliptic restricted three body problem. If a particle survived the whole integration time at all initial longitudes, then the system was classified as stable. For circumbinary orbits, and by using a least squares fit to their data, they obtained an expression for the critical planetary semimajor axis  $a_c$ , i.e. the smallest planetary semi-major axis for which the particles were stable at all initial positions, given by (using our notation for the mass parameters and orbital elements):

$$a_c = [(1.60 \pm 0.04) + (5.10 \pm 0.05)e_1 + (-2.22 \pm 0.11)e_1^2 + (4.12 \pm 0.09)\mu_1 + (-4.27 \pm 0.17)e_1\mu_1 + (-5.09 \pm 0.11)\mu_1^2 + (4.61 \pm 0.36)e_1^2\mu_1^2]a_1. \quad (41)$$

Finally, the initial stellar eccentric anomaly and the initial planetary mean anomaly were varied from  $0^\circ$  to  $360^\circ$  with a step of  $45^\circ$ . The results from the numerical simulations were compared with our analytical estimates for  $\langle e_2^2 \rangle$  and  $e_2^{max}$ , i.e. equations (38) and (40), on both short and secular timescales. For the short timescale simulations the integration time was one planetary orbital period, while for the long term simulations the integration time was set to  $2\pi/(K_1 - K_3)$ , which is the analytical estimate for the secular period of the planetary eccentricity.

Generally, our analytical estimates were in good agreement with the results obtained from the numerical simulations. As expected, the greatest errors were for systems where the planet was started at the critical semi-major axis. As we move away from the critical semi-major axis the error reduces rapidly. Figures 2-5 show the most relevant numerical findings. Finally, Figure 6 is an example that demonstrates the validity of our assumption that the semi-major axes and stellar eccentricity remain constant.

#### 4. POST-NEWTONIAN CORRECTION

For certain stellar binaries the gravitational field between the two stars can be strong enough to make it necessary to include General Relativity in order to describe the motion of the system correctly. In such cases, our theory can easily be modified to account for the extra perturbation. One simply adds the following first order post-Newtonian correction for the stellar orbit to the equation (2) (e.g. Naoz et al. 2013b):

$$H_{1PN} = -\frac{(m_0^3 + m_1^3)p^4}{8c^2m_0^3m_1^3} - \frac{\mathcal{G}(3m_0^2 + 7m_0m_1 + 3m_1^2)p^2}{2c^2m_0m_1r} - \frac{\mathcal{G}(\mathbf{p} \cdot \mathbf{r})^2}{2c^2r^3} + \frac{\mathcal{G}^2(m_0 + m_1)^2m}{2c^2r^2}, \quad (42)$$

where  $\mathbf{p}$  and  $p$  are the linear momentum and its magnitude respectively and  $c$  is the speed of light in vacuum. Averaging the above Hamiltonian over the fast motion, we obtain (Naoz et al. 2013b):

$$\langle H_{1PN} \rangle = \frac{\mathcal{G}^4m_0^5m_1^5(15m_0^2 + 29m_0m_1 + 15m_1^2)}{8(m_0 + m_1)^3c^2L_{1l}^4} - \frac{3\mathcal{G}^4m_0^5m_1^5}{(m_0 + m_1)c^2L_{1l}^3G_{1l}} \quad (43)$$

which eventually results in having the following extra term:

$$\frac{dg_{1PN}}{dt} = \frac{3\mathcal{G}^{\frac{3}{2}}(m_0 + m_1)^{\frac{3}{2}}}{c^2a_{1l}^{\frac{5}{2}}(1 - e_{1l}^2)}. \quad (44)$$

The above term can simply be added to equation (15). Then we have

$$\frac{dg_1}{dt} \approx \frac{dg_{1l}}{dt} + \frac{dg_{1PN}}{dt} \quad (45)$$

and consequently

$$g_1(t) \approx K_{3PN} t \quad (46)$$

where

$$K_{3PN} = \frac{3\mathcal{G}^{\frac{1}{2}}m_2a_{1l}^{\frac{3}{2}}(1 - e_{1l}^2)^{\frac{1}{2}}}{4(m_0 + m_1)^{\frac{1}{2}}a_{2l}^3} + \frac{3\mathcal{G}^{\frac{3}{2}}(m_0 + m_1)^{\frac{3}{2}}}{c^2a_{1l}^{\frac{5}{2}}(1 - e_{1l}^2)}. \quad (47)$$

An example of the effect of the post-newtonian (PN) correction is given in Figure 7.

Here, we have integrated numerically the Einstein-Infeld-Hoffmann equations using a

Gauss-Radau scheme (Eggl & Dvorak 2010) for a system with  $m_0 = 5M_\odot$ ,  $m_1 = 4M_\odot$ ,  $m_2 = 1M_J$ ,  $a_1 = 0.2$  au,  $e_1 = 0.5$ ,  $\varpi = 0^\circ$ ,  $E_{10} = 0^\circ$  and  $l_{20} = 90^\circ$ . The initial period ratio for the above system was  $X=200$ , yielding a planetary semi-major axis  $a_2 = 6.84014558$  au. The graph demonstrates that the inclusion of GR in modelling the motion of the stellar binary can have a significant effect on the evolution of the planetary eccentricity.

The post-Newtonian correction can be applied to our analytic estimates by simply exchanging  $K_3$  with  $K_{3PN}$ , for instance, in equations (35) and (38) - (40).

## 5. ANALYTIC DESCRIPTION OF THE SYSTEM'S EVOLUTION

In this section we demonstrate how equations (22), (35) and (46) can be used to describe the time evolution of the entire system, i.e. the binary and the planet. For the inner orbit we have

$$\varpi_1 \approx g_1 = K_{3PN}t, \quad (48)$$

$$l_1 = n_1t + l_{10}, \quad (49)$$

$$r \cos f_1 = a_1(\cos E_1 - e_1), \quad (50)$$

$$r \sin f_1 = a_1(1 - e_1^2)^{1/2} \sin E_1, \quad (51)$$

where  $f_1$  denotes the corresponding true anomaly. Here we have assumed that  $\dot{a}_1 = \dot{e}_1 = 0$ . For the mean motion follows that  $n_1 = \mathcal{G}^{1/2}(m_0 + m_1)^{1/2}a_1^{-3/2}$ . Defining  $\mathbf{W}_i$  as the simple 2D rotation matrix

$$\mathbf{W}_i = \begin{pmatrix} \cos \varpi_i & -\sin \varpi_i \\ \sin \varpi_i & \cos \varpi_i \end{pmatrix}, \quad i = 1, 2 \quad (52)$$

we find the solution for the relative vector of the binary stars,  $\mathbf{r}(t)$  is

$$\mathbf{r} = \mathbf{W}_1(r \cos f_1, r \sin f_1)^T. \quad (53)$$

In order to find the position vector of the planet, one follows the same procedure, except now the length of the eccentricity vector is no longer constant in time and we have

$$\varpi_2 = \arctan(e_{22}/e_{21}), \quad (54)$$

$$l_2 = n_2 t + \varpi_2 + l_{20}, \quad (55)$$

$$e_2(t) = |\mathbf{e}_2|(t), \quad (56)$$

$$R \cos f_2 = a_2(\cos E_2 - e_2), \quad (57)$$

$$R \sin f_2 = a_2(1 - e_2^2)^{1/2} \sin E_2, \quad (58)$$

where  $n_2 = (\mathcal{G}M)^{1/2} a_2^{-3/2}$ . Here, the corresponding values for  $\mathbf{e}_2$  have to be taken from equations (35). The relative vector from the barycenter of the binary star to the planet is then given by

$$\mathbf{R} = \mathbf{W}_2(R \cos f_2, R \sin f_2)^T. \quad (59)$$

Again, we have assumed that  $\dot{a}_2 = 0$ . We would like to point out here that the eccentric anomaly  $E_i$  for any of the two orbits can be computed by solving Kepler's equation  $l_i = E_i - e_i \sin E_i$ . Alternatively, a series expansion that relates the mean and the true anomaly could be used, for instance (e.g see Murray & Dermott 1999):

$$f_i = l_i + 2e_i \sin l_i + \frac{5}{4}e_i^2 \sin 2l_i + O(e_i^3) \quad (60)$$

However, one should keep in mind that the above series solution is divergent for  $e_i > 0.6627434$ .

A transformation to barycentric coordinates can be easily achieved through

$$\mathbf{r}_{0b} = -\frac{m_1}{m_0 + m_1} \mathbf{r} - \frac{m_2}{M} \mathbf{R} \quad (61)$$

$$\mathbf{r}_{1b} = \frac{m_0}{m_0 + m_1} \mathbf{r} - \frac{m_2}{M} \mathbf{R} \quad (62)$$

$$\mathbf{r}_{2b} = \frac{m_1 + m_2}{M} \mathbf{R}, \quad (63)$$

where  $\mathbf{r}_{ib}$  is the vector of the  $m_i$  body with respect to the system's barycentre.

## 6. APPLICATIONS TO REAL SYSTEMS

We now apply our analytical theory to real circumbinary planetary systems. For that purpose, the Kepler-16, Kepler-34, Kepler-35, Kepler-38, Kepler-64 and Kepler-413 systems were selected, as they are currently believed to harbour only one planet in a circumbinary orbit. The systems are assumed to be coplanar,  $\varpi_1 = 0^\circ$ ,  $E_{10} = 0^\circ$  and  $l_{20} = 90^\circ$ , while the rest of the system parameters were taken from the corresponding discovery papers (Doyle et al. 2011; Welsh et al. 2012; Orosz et al. 2012; Schwamb et al. 2013; Kostov et al. 2014). The systems were integrated over one analytical secular period and no other effects than Newtonian gravity were considered, as they were not expected to make a significant contribution to the systems under investigation (e.g. Chavez et al. 2015). Table 1 gives the mass parameters and orbital elements of each system.

Figures 8 and 9 show the results for the six Kepler systems. Generally, the numerical results are in good agreement with the analytical estimates. Furthermore, one can see that for most planets the current state of eccentricities, indicated by a black horizontal line, is compatible with formation scenarios that predict initial orbits with low eccentricities after the gaseous phase. As in-situ planetesimal accretion as well as gravitational collapse have practically been ruled out for most of the circumbinary planets discovered during the Kepler mission (e.g. Pelupessy & Portegies Zwart 2013; Lines et al. 2014), a fast disc driven migration with little time spent near resonances seems to be the most likely formation scenario for Kepler-16, Kepler-35, Kepler-38 and Kepler-64 (e.g. Kley & Haghighipour 2014).

Exceptions are Kepler-34 and Kepler-413, both with a higher planetary eccentricity of  $e_2 = 0.182$  and  $e_2 = 0.1181$ , respectively. Looking at the relevant plots, it is clear that starting the planet on a circular orbit can not produce a planetary orbit with eccentricities higher than 0.03 for Kepler-34b and 0.04 for Kepler-413b. Moreover, the main eccentricity

contribution for both systems comes from short period activity. This is to be expected, as the stellar masses of Kepler-34 have only around 2.5% difference, and the stellar eccentricity of the Kepler-413 is just 0.0365. As a result, the forced secular eccentricity, which is proportional to the difference between the masses of the stellar components and to the stellar eccentricity is very small. Therefore, either those two planets were formed on a non-circular orbit or if they were initially circular, some dynamical event may have taken place and pumped up their eccentricity. For instance, an as of yet undetected companion as well as an encounter with another star may have injected eccentricity into the planet’s orbit. Such an interaction would also explain the slight misalignment of the orbital planes in Kepler-413. Another possible explanation for the elevated Kepler-34b is resonance trapping. If the planet’s migration has not been fast enough, the planet may be trapped in a resonance which can cause a significant increase in its orbital eccentricity (Kley & Haghighipour 2014). In the case of Kepler-34b the 10:1 mean motion resonance with the stellar binary may have affected the evolution of the planetary eccentricity to some extent (Chavez et al. 2015).

## 7. DISCUSSION

We would like to point out here that we assumed our six Kepler systems to be coplanar. In reality, they all have some mutual orbital inclination, with Kepler-413 having the largest one among those systems, i.e.  $I = 4.073^\circ$ . In order to check whether our analytic description of the system’s evolution remains valid for such inclinations, we ran two and three dimensional simulations for Kepler-413. We found that difference between the two models was insignificant for the amplitude of the eccentricity vector. Therefore, our predictions for the maximum and average eccentricities remain valid. However, the longitude of pericentre seemed to be affected considerably. Hence, we do not recommend to

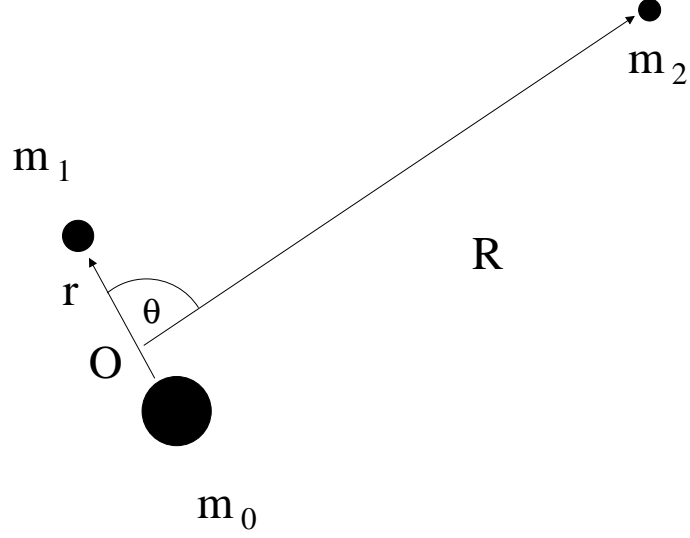


Fig. 1.— The Jacobi decomposition of the three body problem.

Table 1: Masses and orbital elements for Kepler-16, Kepler-34, Kepler-35, Kepler-38, Kepler-64 and Kepler-413.

System	$m_0(M_\odot)$	$m_1(M_\odot)$	$m_2(M_J)$	$a_1$ (au)	$a_2$ (au)	$e_1$
Kepler-16	$0.6897^{+0.0035}_{-0.0034}$	$0.20255^{+0.00066}_{-0.00065}$	$0.333^{+0.016}_{-0.016}$	$0.22431^{+0.00035}_{-0.00034}$	$0.7048^{+0.0011}_{-0.0011}$	$0.15944^{+0.00061}_{-0.00062}$
Kepler-34	$1.0479^{+0.0033}_{-0.0030}$	$1.0208^{+0.0022}_{-0.0022}$	$0.220^{+0.011}_{-0.010}$	$0.22882^{+0.00019}_{-0.00018}$	$1.0896^{+0.0009}_{-0.0009}$	$0.52087^{+0.00052}_{-0.00055}$
Kepler-35	$0.8876^{+0.0051}_{-0.0053}$	$0.8094^{+0.0041}_{-0.0044}$	$0.127^{+0.020}_{-0.021}$	$0.17617^{+0.00028}_{-0.00029}$	$0.60345^{+0.00100}_{-0.00102}$	$0.1421^{+0.0014}_{-0.0014}$
Kepler-38	0.949	0.249	<0.384 (95% conf.)	0.1469	0.4644	0.1032
Kepler-64	$1.384^{+0.079}_{-0.079}$	$0.386^{+0.018}_{-0.018}$	<0.532 (99.7% conf.)	$0.1744^{+0.0031}_{-0.0031}$	$0.634^{+0.011}_{-0.011}$	$0.2117^{+0.0051}_{-0.0051}$
Kepler-413	0.820	0.5423	0.21	0.10148	0.3553	0.0365



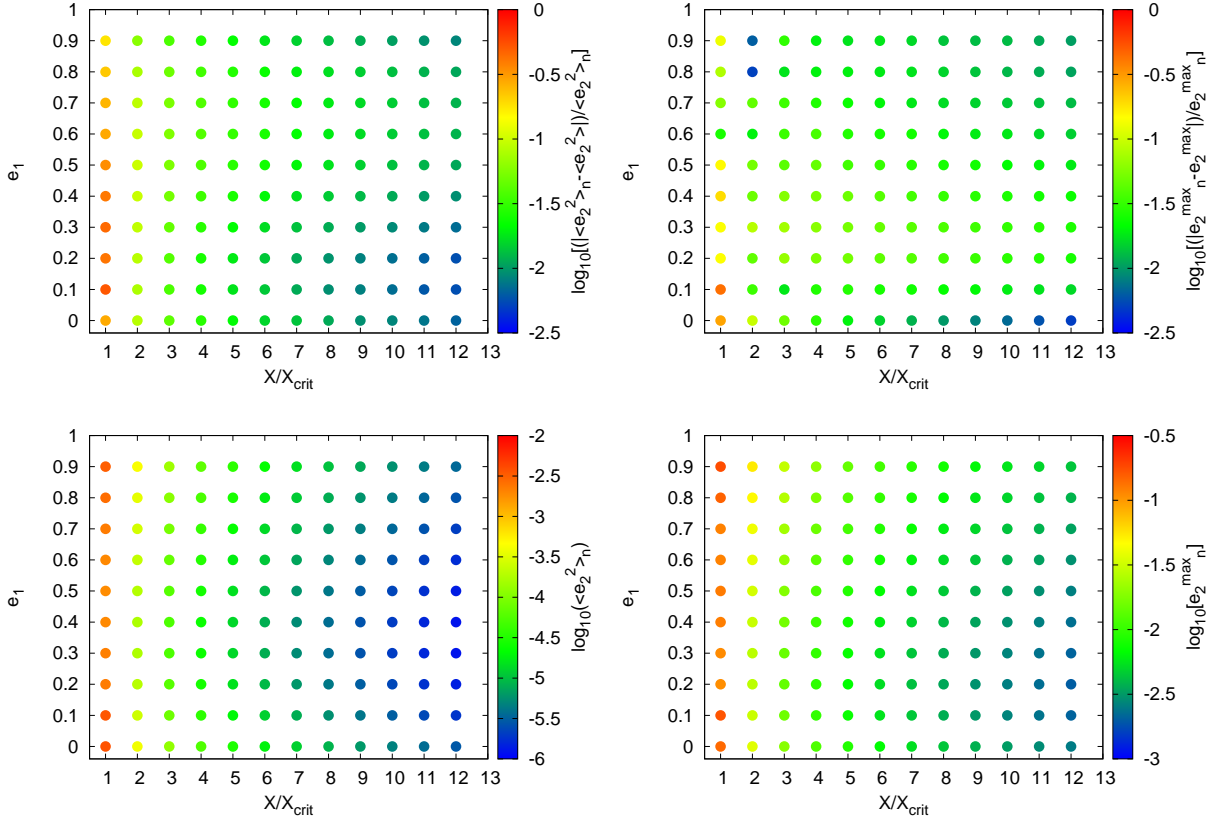


Fig. 2.— Top row: logarithmic error (in color) for the averaged square planetary eccentricity (left) and the maximum planetary eccentricity (right). Bottom row: the logarithms of the numerical values (in colour) of the averaged squared planetary eccentricity (left) and the maximum planetary eccentricity (right). The mass parameters of the system are  $m_1/(m_0 + m_1) = 0.5$  and  $m_2/(m_0 + m_1) = 10^{-2}$ ,  $X$  is the initial period ratio and  $X_{crit}$  is the critical period ratio based on Holman & Wiegert (1999). The integration time is one planetary orbital period.

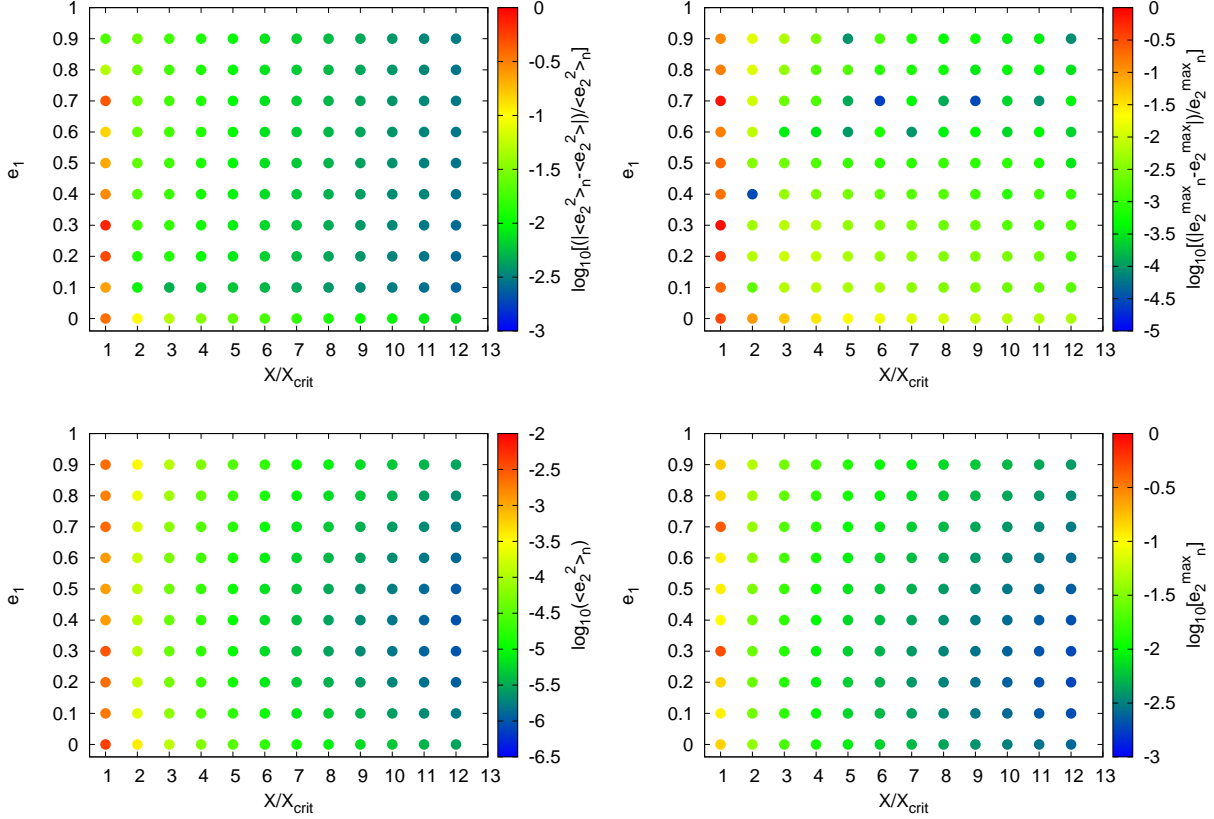


Fig. 3.— Top row: logarithmic error (in color) for the averaged square planetary eccentricity (left) and the maximum planetary eccentricity (right). Bottom row: the logarithms of the numerical values (in colour) of the averaged squared planetary eccentricity (left) and the maximum planetary eccentricity (right). The mass parameters of the system are  $m_1/(m_0 + m_1) = 0.3$  and  $m_2/(m_0 + m_1) = 10^{-3}$ ,  $X$  is the initial period ratio and  $X_{crit}$  is the critical period ratio based on Holman & Wiegert (1999). The integration time is one analytical secular period.

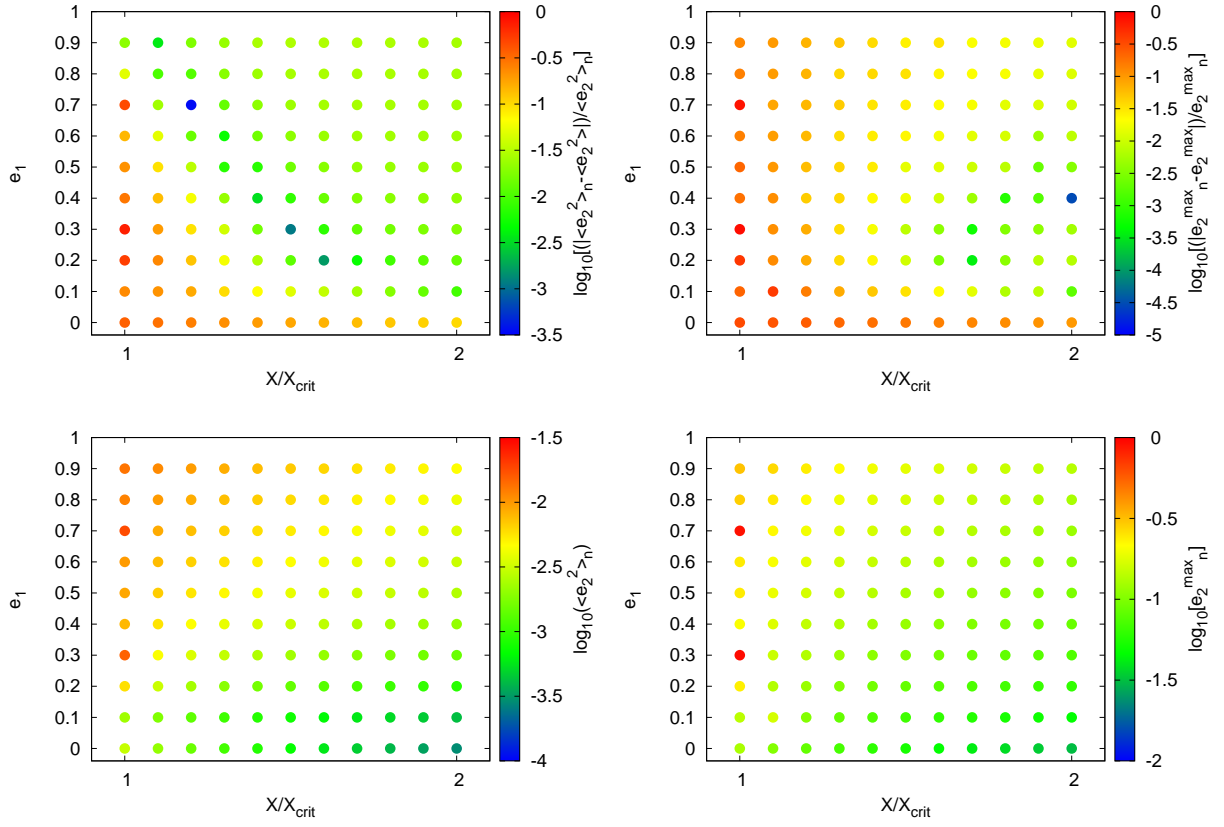


Fig. 4.— A zoom in of the plots of Figure 3 for  $1 \leq X/X_{crit} \leq 2$ .

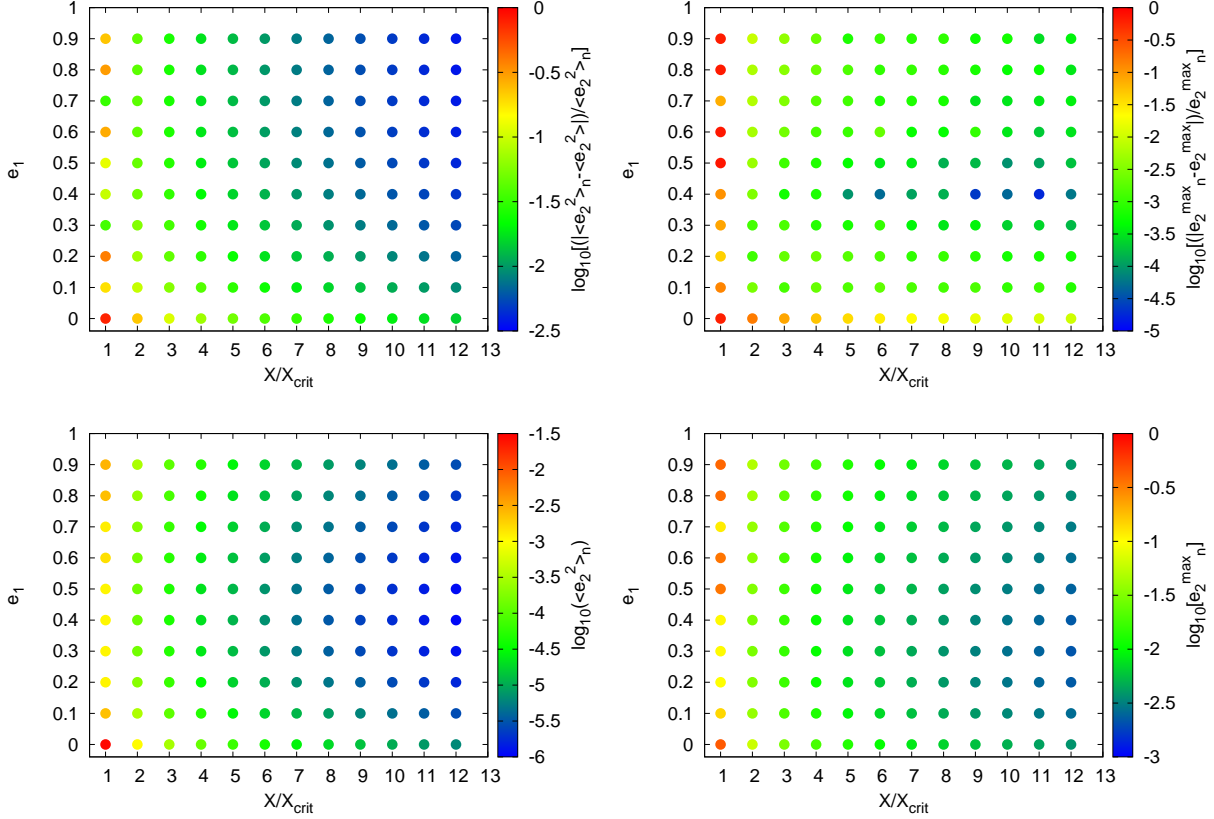


Fig. 5.— Top row: logarithmic error (in color) for the averaged square planetary eccentricity (left) and the maximum planetary eccentricity (right). Bottom row: the logarithms of the numerical values (in colour) of the averaged squared planetary eccentricity (left) and the maximum planetary eccentricity (right). The mass parameters of the system are  $m_1/(m_0 + m_1) = 0.1$  and  $m_2/(m_0 + m_1) = 10^{-6}$ ,  $X$  is the initial period ratio and  $X_{crit}$  is the critical period ratio based on Holman & Wiegert (1999). The integration time is one analytical secular period.

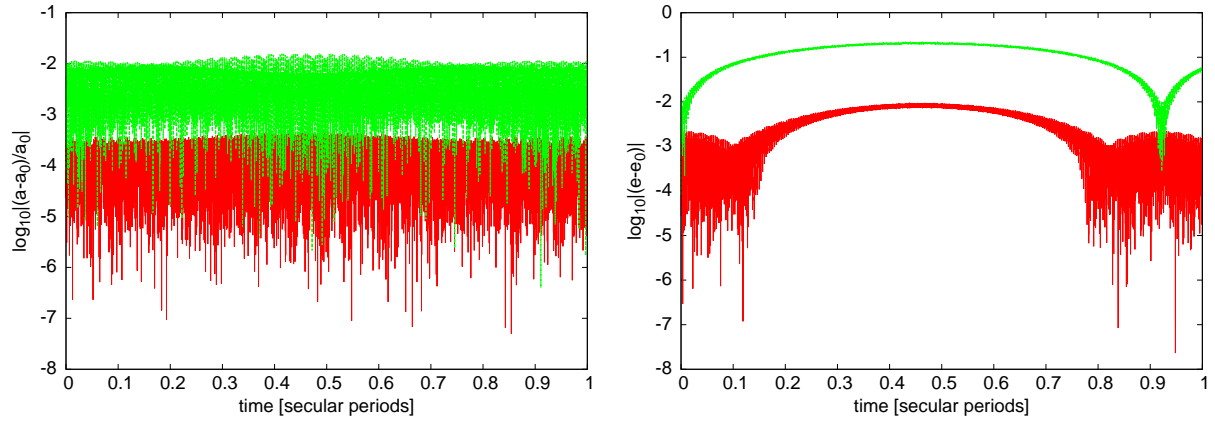


Fig. 6.— Semi-major axis logarithmic relative change (left graph) and logarithmic absolute change in the eccentricity (right graph). The red colour represents the stellar orbit, while the green colour represents the planetary orbit. The mass parameters of the system are  $m_1/(m_0 + m_1) = 0.1$  and  $m_2/(m_0 + m_1) = 10^{-2}$ , the initial stellar eccentricity is 0.5, the initial stellar eccentric anomaly is  $0^\circ$ , the initial planetary mean anomaly is  $90^\circ$ , the initial period ratio is  $1.5X_{crit}$  and the integration time is one analytical secular period. Variations in the planetary eccentricity remain dominant even for systems close to the critical period ratio for dynamical instability.

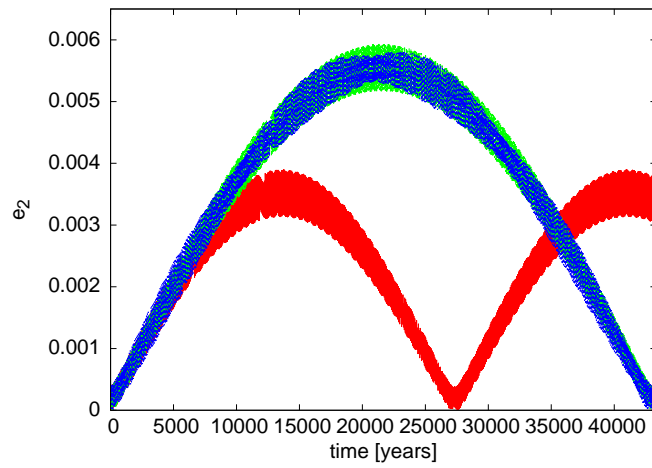


Fig. 7.— Eccentricity against time for for a system with  $m_0 = 5M_\odot$ ,  $m_1 = 4M_\odot$ ,  $m_2 = 1M_J$ ,  $a_1 = 0.2$  au,  $a_2 = 6.84014558$  au,  $e_1 = 0.5$ ,  $\varpi_1 = 0^\circ$ ,  $E_{10} = 0^\circ$  and  $l_{20} = 90^\circ$ . The red curve comes from the integration of the non-relativistic full equations of motion, the green curve comes from the integration of the relativistic full equations of motion and the blue curve is our analytic estimate.

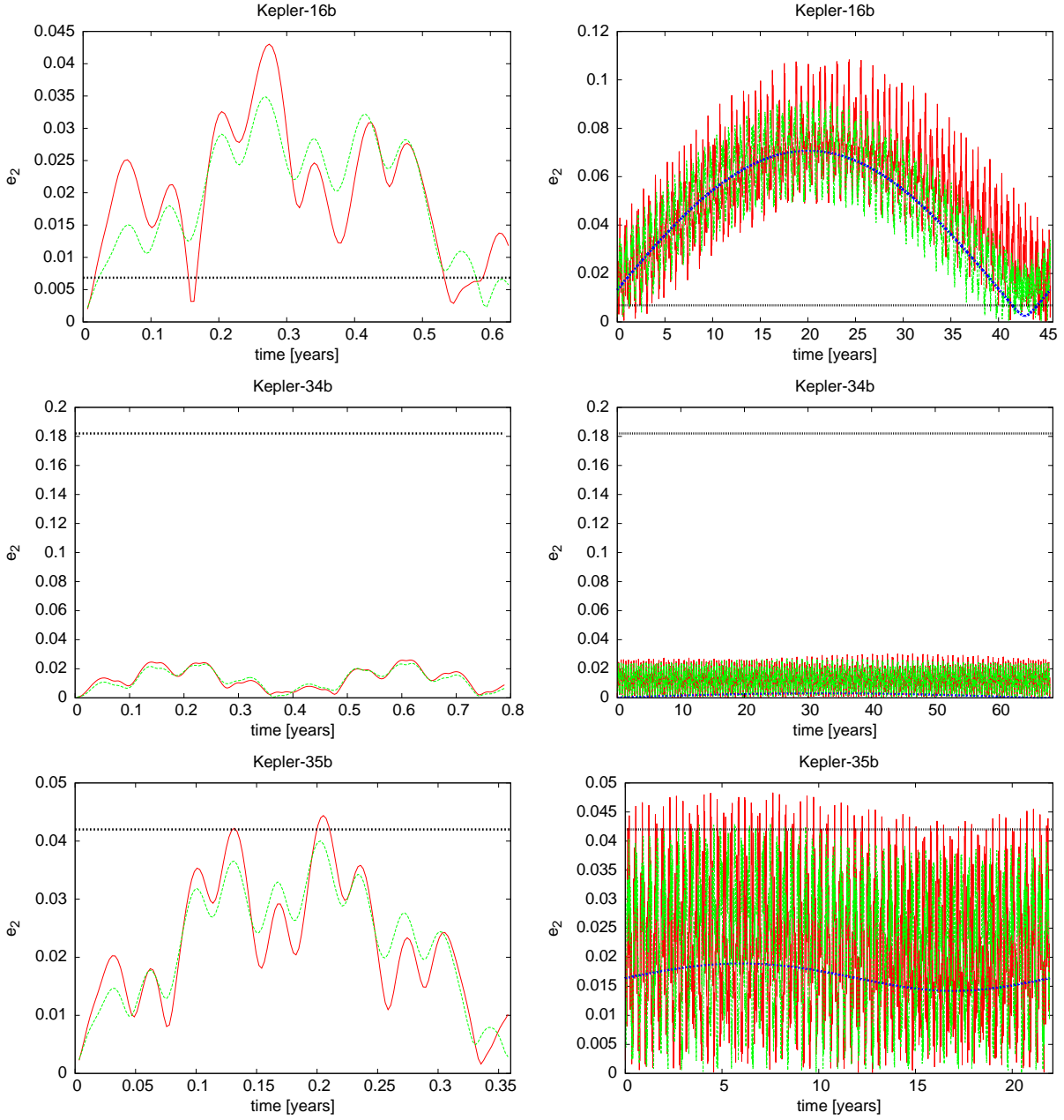


Fig. 8.— Eccentricity against time for Kepler-16b, Kepler-34b and Kepler-35b. The red curve comes from the numerical integration of the full equations of motion, the green curve is our analytical estimates, the blue curve is the analytical secular solution, while the black line denotes the current value of the planetary eccentricity. The integration time is one planetary period for the left column and one analytical secular period for the right column.

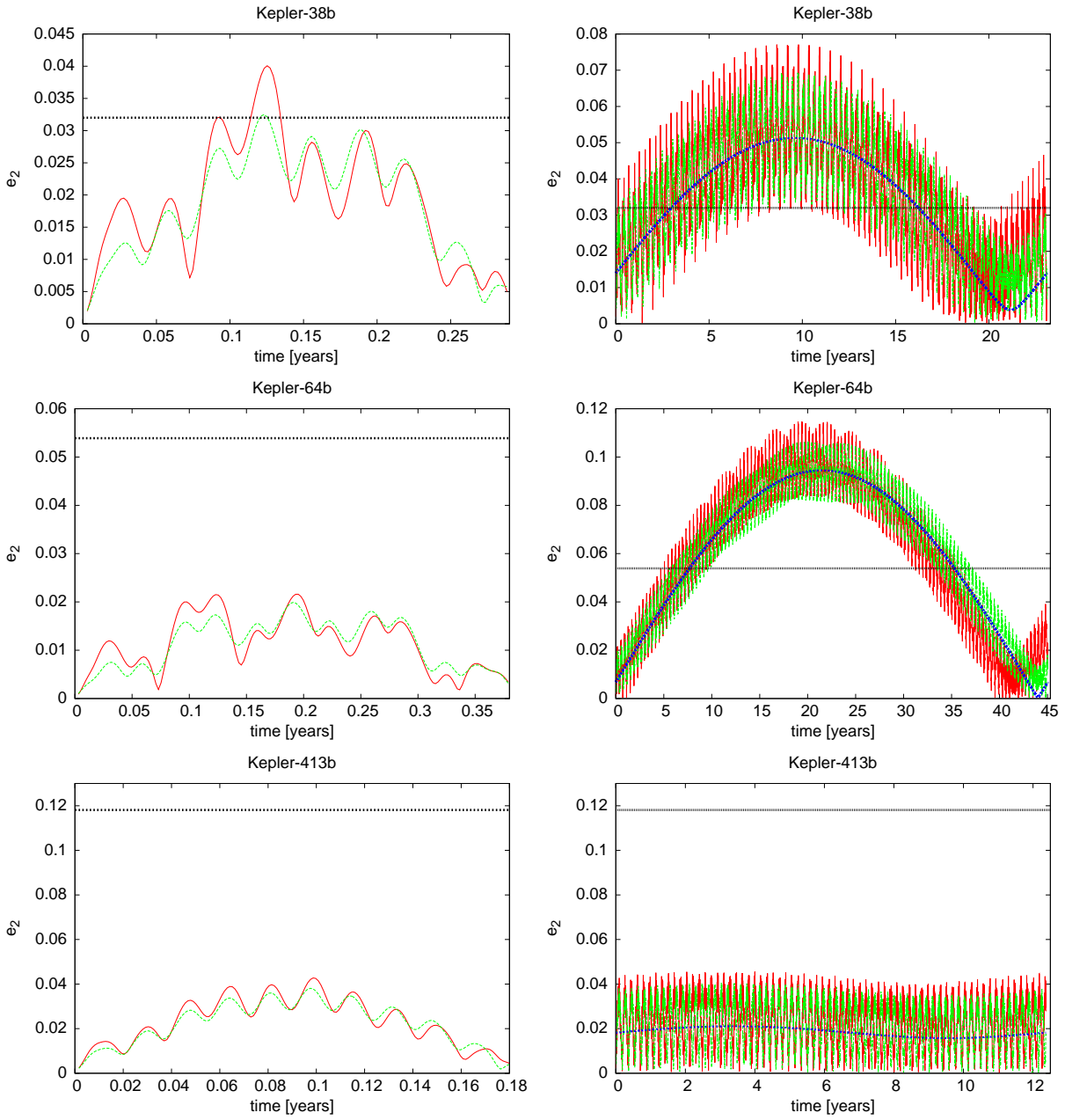


Fig. 9.— Same as Figure 8, but for Kepler-38b, Kepler-64b and Kepler-413b.



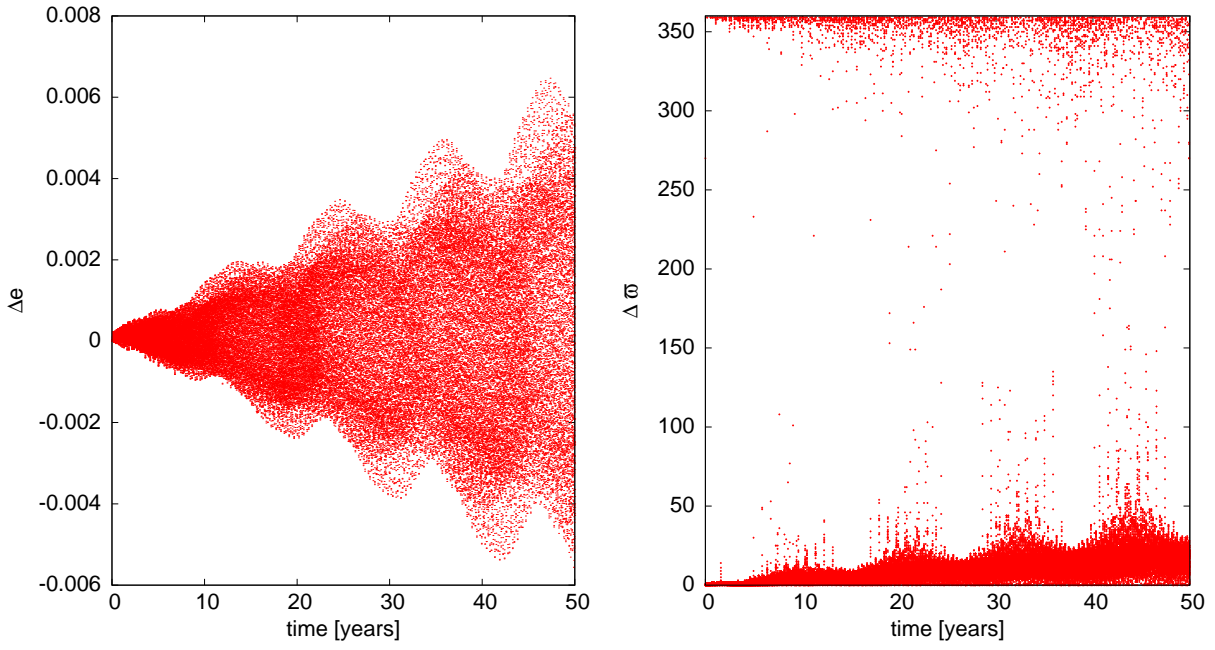


Fig. 10.— Difference in the eccentricity (left) and in the longitude of pericentre (right) between a 2D and a 3D model of Kepler-413. See Figure 9 for a comparison with the current and predicted eccentricity estimates. The secular period for a coplanar planetary orbit is about 12 years.

use the fully analytic description presented in section 5 to describe a system’s long term orbit evolution for mutual inclinations around  $I \approx 5^\circ$  or higher. Figure 9 presents the relevant information.

## 8. SUMMARY

In this work, we derived analytical estimates for the motion of coplanar circumbinary planets. The derivation was done for initially circular orbits and it assumed that the planetary eccentricity remains low ( $e_2 < 0.2$ ). Short term motion was described by solving differential equations derived from the Runge-Lenz vector. Similarly, canonical perturbation theory was used to model the secular motion. Working with the eccentric instead of the true anomaly to describe the short term motion of the perturber leads to a solution that does not depend on a series expansion in terms of the eccentricity of the binary. This is a great advantage as we do not need to worry about the convergence of the solution and the magnitude of the eccentricity of the perturber. Hence, our derivations are valid for all eccentricities of the stellar binary as long as the planet is far enough from the binary so that a hierarchical triple system can be considered.

In section 5 we have presented a complete analytical framework to describe the motion of a stellar binary and its circumbinary planet. Analytical expressions were derived for the averaged square eccentricity as well as for the maximum value of the planet’s eccentricity. The estimates were tested numerically for different stellar and planetary masses over a wide range of eccentricity and period ratios. The results showed very good agreement between the numerical simulations and the analytical estimates. Furthermore, in case it is required, the analytical formulae can easily be adjusted to incorporate some general relativistic effects. Finally, the analytical estimates were applied to six Kepler circumbinary systems with good results, as they provided valuable information about the evolution and possibly the

formation of those systems.

The analytical estimates obtained in this work can be used, for instance, in analytic planet formation theories, in modelling transits in circumbinary planetary systems, or determining habitable zones around stellar binaries.

S.E. is grateful for the support by the European Union Seventh Framework Program (FP7/2007-2013) under grant agreement no. 282703, as well as the travel funding by the Austrian FWF project S11608-N16 (sub-project of the NFN S116).

## APPENDIX

The expressions for  $P_1(t)$  and  $P_2(t)$  in equations (31) are presented. They contain the short periodic terms of the outer eccentric vector. For  $t = t_0$  we have  $E_1 = E_{10}$  and  $l_2 = l_{20}$ .

$$\begin{aligned}
P_1(t) = & \frac{21}{32}(1 - \sqrt{1 - e_1^2}) \cos(2E_1 + 3l_2) + \frac{3}{32}(1 - \sqrt{1 - e_1^2}) \cos(2E_1 + l_2) - \frac{3}{32}(1 + \\
& + \sqrt{1 - e_1^2}) \cos(2E_1 - l_2) - \frac{21}{32}(1 + \sqrt{1 - e_1^2}) \cos(2E_1 - 3l_2) + e_1 \left[ -\frac{21}{96}(1 - \right. \\
& - \sqrt{1 - e_1^2}) \cos(3E_1 + 3l_2) - \frac{3}{96}(1 - \sqrt{1 - e_1^2}) \cos(3E_1 + l_2) + \frac{3}{32}(13 + \\
& + 5\sqrt{1 - e_1^2}) \cos(E_1 - l_2) + \frac{3}{96}(1 + \sqrt{1 - e_1^2}) \cos(3E_1 - l_2) - \frac{105}{32}(1 - \\
& - \sqrt{1 - e_1^2}) \cos(E_1 + 3l_2) + \frac{21}{96}(1 + \sqrt{1 - e_1^2}) \cos(3E_1 - 3l_2) - \frac{3}{32}(13 - \\
& - 5\sqrt{1 - e_1^2}) \cos(E_1 + l_2) + \left. \frac{105}{32}(1 + \sqrt{1 - e_1^2}) \cos(E_1 - 3l_2) \right] + e_1^2 \left[ \frac{3}{32} \left( \frac{7}{2} - \right. \right. \\
& - \sqrt{1 - e_1^2}) \cos(2E_1 + l_2) + \frac{21}{32} \left( \frac{1}{2} - \sqrt{1 - e_1^2} \right) \cos(2E_1 + 3l_2) - \frac{3}{32} \left( \frac{7}{2} + \right. \\
& + \sqrt{1 - e_1^2}) \cos(2E_1 - l_2) - \left. \frac{21}{32} \left( \frac{1}{2} + \sqrt{1 - e_1^2} \right) \cos(2E_1 - 3l_2) \right] + e_1^3 \left[ -\frac{1}{64} \times \right. \\
& \times \cos(3E_1 + l_2) - \frac{7}{64} \cos(3E_1 - 3l_2) + \frac{3}{64} \cos(E_1 - l_2) + \frac{7}{64} \cos(3E_1 + 3l_2) + \\
& + \frac{21}{64} \cos(E_1 + 3l_2) - \frac{3}{64} \cos(E_1 + l_2) + \frac{1}{64} \cos(3E_1 - l_2) - \\
& \left. - \frac{21}{64} \cos(E_1 - 3l_2) \right] \tag{64}
\end{aligned}$$

$$\begin{aligned}
P_2(t) = & \frac{21}{32}(1 - \sqrt{1 - e_1^2}) \sin(2E_1 + 3l_2) - \frac{3}{32}(1 - \sqrt{1 - e_1^2}) \sin(2E_1 + l_2) - \frac{3}{32}(1 + \\
& + \sqrt{1 - e_1^2}) \sin(2E_1 - l_2) + \frac{21}{32}(1 + \sqrt{1 - e_1^2}) \sin(2E_1 - 3l_2) + e_1 \left[ -\frac{7}{32}(1 - \right. \\
& - \sqrt{1 - e_1^2}) \sin(3E_1 + 3l_2) + \frac{1}{32}(1 - \sqrt{1 - e_1^2}) \sin(3E_1 + l_2) - \frac{3}{32}(3 - \\
& - 5\sqrt{1 - e_1^2}) \sin(E_1 - l_2) + \frac{1}{32}(1 + \sqrt{1 - e_1^2}) \sin(3E_1 - l_2) - \frac{105}{32}(1 - \\
& - \sqrt{1 - e_1^2}) \sin(E_1 + 3l_2) - \frac{7}{32}(1 + \sqrt{1 - e_1^2}) \sin(3E_1 - 3l_2) - \frac{3}{32}(3 + \\
& + 5\sqrt{1 - e_1^2}) \sin(E_1 + l_2) - \left. \frac{105}{32}(1 + \sqrt{1 - e_1^2}) \sin(E_1 - 3l_2) \right] + e_1^2 \left[ \frac{3}{32} \left( \frac{5}{2} + \right. \right. \\
& + \sqrt{1 - e_1^2}) \sin(2E_1 + l_2) + \frac{21}{32} \left( \frac{1}{2} - \sqrt{1 - e_1^2}) \sin(2E_1 + 3l_2) + \frac{3}{32} \left( \frac{5}{2} - \right. \\
& - \sqrt{1 - e_1^2}) \sin(2E_1 - l_2) + \left. \left. \frac{21}{32} \left( \frac{1}{2} + \sqrt{1 - e_1^2}) \sin(2E_1 - 3l_2) \right) \right] + e_1^3 \left[ -\frac{3}{64} \times \right. \\
& \times \sin(3E_1 + l_2) + \frac{7}{64} \sin(3E_1 - 3l_2) - \frac{9}{64} \sin(E_1 - l_2) + \frac{7}{64} \sin(3E_1 + 3l_2) + \\
& + \frac{21}{64} \sin(E_1 + 3l_2) - \frac{9}{64} \sin(E_1 + l_2) - \frac{3}{64} \sin(3E_1 - l_2) + \\
& \left. + \frac{21}{64} \sin(E_1 - 3l_2) \right] \tag{65}
\end{aligned}$$

## NOTATION

$a_i$	semimajor axis of the inner ( $i = 1$ ) and outer ( $i = 2$ ) orbit
$c$	vacuum light speed
$C$	integration constants
$e_i$	eccentricity vectors
$e_{ij}$	x ( $j = 1$ ) and y ( $j = 2$ ) components of the inner and outer eccentricity vector
$E_i$	eccentric anomalies
$f_i$	true anomalies
$\mathcal{G}$	gravitational constant
$h$	specific angular momentum of the outer orbit
$H$	Hamiltonians
$I$	mutual inclination of the binary and planetary orbits
$K_i$	parameters of the long term solution
$L_i, G_i$	Delaunay actions
$l_i, g_i$	Delaunay angles (mean anomaly, argument of pericenter)
$m_0, m_1$	masses of the two stars
$m_2$	mass of the planet
$M$	total mass of the system
$m, \mathcal{M}, M_j, \mu_i$	mass parameters
$n_i$	mean motions
$\mathcal{P}_n$	Legendre polynomials
$P_i$	x and y component terms of short period $\mathbf{e}_2$ solution
$\mathbf{r}_{ib}$	barycentric position vectors of the stars ( $i = 0, 1$ ) and the planet ( $i = 2$ )
$\mathbf{r}$	Jacobi vector of the stellar orbit
$\mathbf{R}$	Jacobi vector of the planetary orbit
$\theta$	angle between $\mathbf{r}$ and $\mathbf{R}$
$t$	time
$\varpi_i$	stellar and planetary longitude of pericentre
$\mathbf{W}_i$	pericentre rotation matrices
$X$	period ratio between outer and inner orbit

## REFERENCES

- Blaes, O., Lee, M. H., & Socrates, A. 2002, *ApJ*, 578, 775
- Borkovits, T., Forgács-Dajka, E., & Regály, Z. 2007, *A&A*, 473, 191
- Brouwer, D. 1959, *AJ*, 64, 378
- Chavez, C. E., Georgakarakos, N., Prodan, S., et al. 2015, *MNRAS*, 446, 1283
- Chavez, C. E., Tovmassian, G., Aguilar, L. A., Zharikov, S., & Henden, A. A. 2012, *A&A*, 538, A122
- Demidova, T. V., & Shevchenko, I. I. 2014, *ArXiv e-prints*, arXiv:1407.5493
- Doyle, L. R., Carter, J. A., Fabrycky, D. C., et al. 2011, *Science*, 333, 1602
- Eggl, S., & Dvorak, R. 2010, in *Lecture Notes in Physics*, Berlin Springer Verlag, Vol. 790, *Lecture Notes in Physics*, Berlin Springer Verlag, ed. J. Souchay & R. Dvorak, 431–480
- Eggl, S., Pilat-Lohinger, E., Funk, B., Georgakarakos, N., & Haghhighipour, N. 2013, *MNRAS*, 428, 3104
- Eggl, S., Pilat-Lohinger, E., Georgakarakos, N., Gyergyovits, M., & Funk, B. 2012, *ApJ*, 752, 74
- Farago, F., & Laskar, J. 2010, *MNRAS*, 401, 1189
- Ford, E. B., Kozinsky, B., & Rasio, F. A. 2000, *ApJ*, 535, 385
- Georgakarakos, N. 2002, *MNRAS*, 337, 559
- . 2003, *MNRAS*, 345, 340

—. 2004, *Celestial Mechanics and Dynamical Astronomy*, 89, 63

—. 2006, *MNRAS*, 366, 566

—. 2009, *MNRAS*, 392, 1253

Harrington, R. S. 1968, *AJ*, 73, 190

Heppenheimer, T. A. 1978, *A&A*, 65, 421

Holman, M. J., & Wiegert, P. A. 1999, *AJ*, 117, 621

Kaula, W. M. 1962, *AJ*, 67, 300

Kiseleva, L. G., Eggleton, P. P., & Mikkola, S. 1998, *MNRAS*, 300, 292

Kley, W., & Haghighipour, N. 2014, *A&A*, 564, A72

Kostov, V. B., McCullough, P. R., Carter, J. A., et al. 2014, *ApJ*, 784, 14

Kozai, Y. 1962, *AJ*, 67, 591

Krymowski, Y., & Mazeh, T. 1999, *MNRAS*, 304, 720

Lee, M. H., & Peale, S. J. 2003, *ApJ*, 592, 1201

Leung, G. C. K., & Lee, M. H. 2013, *ApJ*, 763, 107

Li, G., Naoz, S., Holman, M., & Loeb, A. 2014, *ApJ*, 791, 86

Lidov, M. L. 1962, *Planet. Space Sci.*, 9, 719

Lines, S., Leinhardt, Z. M., Paardekooper, S., Baruteau, C., & Thebault, P. 2014, *ApJ*, 782,

L11

Liu, B., Muñoz, D. J., & Lai, D. 2015, *MNRAS*, 447, 747



- Liu, X., Baoyin, H., Georgakarakos, N., Donnison, J. R., & Ma, X. 2012, MNRAS, 427, 1034
- Marchal, C. 1990, The three-body problem
- Mazeh, T., & Shaham, J. 1979, A&A, 77, 145
- Mikkola, S. 1997, Celestial Mechanics and Dynamical Astronomy, 67, 145
- Moriwaki, K., & Nakagawa, Y. 2004, ApJ, 609, 1065
- Murray, C. D., & Dermott, S. F. 1999, Solar system dynamics
- Naoz, S., Farr, W. M., Lithwick, Y., Rasio, F. A., & Teyssandier, J. 2013a, MNRAS, 431, 2155
- Naoz, S., Kocsis, B., Loeb, A., & Yunes, N. 2013b, ApJ, 773, 187
- Orosz, J. A., Welsh, W. F., Carter, J. A., et al. 2012, ApJ, 758, 87
- Pelupessy, F. I., & Portegies Zwart, S. 2013, MNRAS, 429, 895
- Schwamb, M. E., Orosz, J. A., Carter, J. A., et al. 2013, ApJ, 768, 127
- Teyssandier, J., Naoz, S., Lizarraga, I., & Rasio, F. A. 2013, ApJ, 779, 166
- Welsh, W. F., Orosz, J. A., Carter, J. A., et al. 2012, Nature, 481, 475